



THE EFFECT OF THE FIBER ORIENTATION ON THE DYNAMIC BEHAVIOUR OF ROTORS IN WOUNDING-SHAFT

José C. Pereira

Universidade Federal de Santa Catarina

Campus Universitário – Trindade – Caixa Postal 476

88040-900 Florianópolis – SC, Brasil - E-mail: jcarlos@grante.ufsc.br

Abstract. *The purpose of this work is to analyse the dynamic behaviour of simple-supported rotors in which its shaft are made of fibre/resin in a winding process. The orientation of the winding angle is an important parameter on determining the properties of the section such as the equivalent bending stiffness $\langle EI \rangle$ and the equivalent torsional stiffness $\langle GJ \rangle$, which can modify the strain energy of the shaft. The Campbell Diagram, in which the bending and torsion modes of the rotor is included, can be appreciably changed with the evolution of the orientation of the winding angle. This analysis can be used in an optimisation process maximizing the critical velocities distance from the operating rotation of the rotor.*

Keywords: *Rotor, Composite, Homogeneity, Campbell Diagram.*

1. INTRODUCTION

In rotordynamics prediction, we currently employ the finite element method to analyse this type of structure in searching the undamped natural frequencies (Campbell Diagram), the steady-state response to unbalance, the transient response to unbalance and external driving forces as shown in Rossi *et al.* (1989). Nelson *et al.* (1976) and Özgüven *et al.* (1984) using the finite element method introduced different effects as the rotatory inertia, gyroscopic moments, axial load, etc. Steffen *et al.* (1987) linked a finite element package with an optimization program in order to perform the optimal structural design with the purpose of to maximizing the distance of the critical speeds from it-selves. In these studies seen earlier the material of the shaft is considered isotropic.

In this work it is introduced a new parameter in rotordynamics analysis given by the fiber orientation in the case of rotors in which the shaft is made of fiber/resin in a winding process. In this case, the homogeneity properties of the cross section of the shaft $\langle EI \rangle$ and $\langle GJ \rangle$ in determining the strain energy in bending and torsion are used. As a first approach, the Rayleigh-Ritz method is used and only the first mode in bending and in torsion are observed

The introduction of the parameter winding angle of the shaft can modify the behaviour in

bending and torsion of the rotor and this effect can be included in optimization techniques in searching the optimal design of the rotor machine.

2. THE EQUATIONS OF ENERGY OF THE ROTOR

2.1 The kinetic energy of the disc

From the Fig. 1, we can deduce the instantaneous vector of rotation in the reference coordinate system, Lalanne *et al.* (1986):

$$\vec{\omega} = \dot{\psi} \vec{z} + \dot{\theta} \vec{x}_1 + \dot{\phi} \vec{y} \quad (1)$$

where \vec{z} , \vec{x}_1 , \vec{y} are unitary vecteurs.

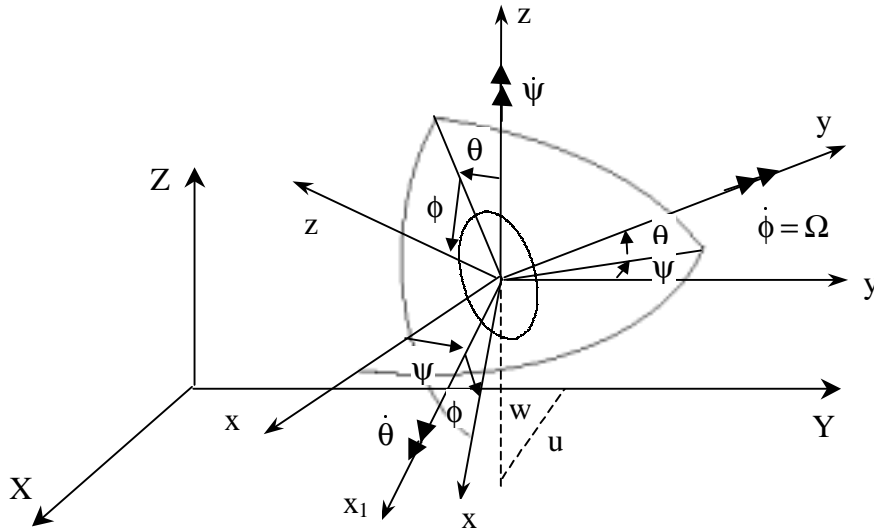


Figure 1- Reference coordinate system (x, y, z)

The angular velocity of the disc is $\dot{\phi}$ and the compounds of $\vec{\omega}$ in the reference coordinate system is:

$$\begin{bmatrix} \omega_x \\ \omega_y \\ \omega_z \end{bmatrix} = \begin{bmatrix} -\dot{\psi} \cos \theta \sin \phi + \dot{\theta} \cos \phi \\ \dot{\phi} + \dot{\psi} \sin \theta \\ \dot{\psi} \cos \theta \cos \phi + \dot{\theta} \sin \phi \end{bmatrix} \quad (2)$$

The kinetic energy of the disc can be expressed by:

$$T_D = \frac{1}{2} M_D (\dot{u}^2 + \dot{w}^2) + \frac{1}{2} (I_{Dz} \omega_z^2 + I_{Dy} \omega_y^2 + I_{Dx} \omega_x^2) \quad (3)$$

where u and w are the coordinates of the center of inertia of the disc and I_{Dx} , I_{Dy} and I_{Dz} are the inertia moments of the disc in the reference coordinate system. Taking in account that the angles θ and ψ are small, the velocity of rotation is $\dot{\phi} = \Omega$ and the symmetry of the disc implies $I_{Dx} = I_{Dz}$, we may obtain from Eq. (3) that:

$$T_D = \frac{1}{2} M_D (\dot{u}^2 + \dot{w}^2) + \frac{1}{2} I_{Dx} (\dot{\theta}^2 + \dot{\psi}^2) + I_{Dy} \Omega \psi \theta + \frac{1}{2} I_{Dy} \Omega^2 \quad (4)$$

From the application of the Eq. (4) in the Lagrange's equation, in which the generalised coordinates are u , w , θ , ψ , we can identify the inertia effect and the gyroscopic effects of the disc.

2.2 The strain energy of the shaft in bending

The general expression for the strain energy is:

$$U = \frac{1}{2} \int_{\tau} \epsilon^t \sigma d\tau \quad (5)$$

where $\sigma = E \epsilon$:

Let be u^* and w^* be components of the displacement of a point P in the cross section in the reference coordinate system, Fig. 2. If we consider only the linear effect of the longitudinal strain:

$$\epsilon_1 = -x \frac{\partial^2 u^*}{\partial y^2} - z \frac{\partial^2 w^*}{\partial y^2} \quad (6)$$

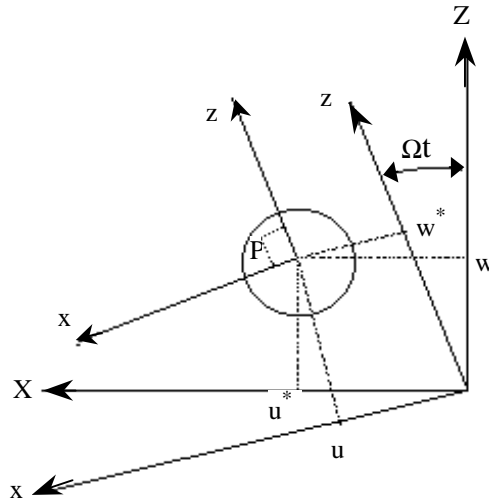


Figure 2 – The reference coordinate system of the shaft

The final expression of the strain energy is:

$$U = \frac{1}{2} E \int_{\tau} \left[-z \frac{\partial^2 w^*}{\partial y^2} - x \frac{\partial^2 u^*}{\partial y^2} \right]^2 d\tau \quad (7)$$

The displacements u^* and w^* in the global coordinate system are:

$$u^* = -w \sin \Omega t + u \cos \Omega t \quad (8)$$

$$w^* = w \cos \Omega t + u \sin \Omega t$$

The Eq. (7) in terms of u and w is:

$$U = \frac{1}{2} E I \int_0^L \left[\left(\frac{\partial^2 w}{\partial y^2} \right)^2 + \left(\frac{\partial^2 u}{\partial y^2} \right)^2 \right] dy \quad (9)$$

From the application of the Eq. (9) in to the Lagrange's equation, in which the generalised coordinates are u , w , we can identify the stiffness of the shaft in bending.

2.3 The movement in torsion of the shaft

The general expression for the kinetic energy of the shaft in torsion is, Lalanne *et al.* (1986):

$$T = \frac{1}{2} \rho J \int_0^L \dot{\phi}^2 dy \quad (10)$$

where ϕ is the torsion angle. The general expression for the strain energy of the shaft in torsion is:

$$U = \frac{1}{2} G J \int_0^L \left(\frac{\partial \phi}{\partial y} \right)^2 dy \quad (11)$$

By using Eq. (10) and Eq. (11) in the Lagrange's equations, in which the generalised coordinate is ϕ , we can deduce the movement of torsion of the shaft.

3. RAYLEIGH-RITZ METHOD

With a reasonable approximation of the displacement field, we can deduce the equations of the movement in bending and in torsion using the Raileigh-Ritz Method. In this work, we search the first frequencies in bending and the first frequency in torsion for a simple-supported rotor, as shown in the Fig. 3.

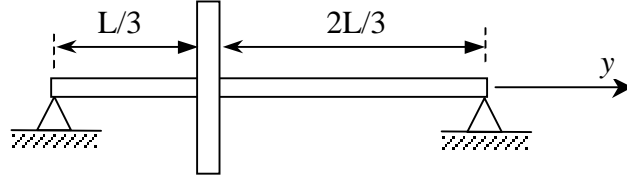


Figure. 3 – Rotor simple-supported on the ends

An approach for the displacement in bending for this configuration is:

$$u(y, t) = \sin \frac{\pi y}{L} p_1 \quad (12)$$

$$w(y, t) = \sin \frac{\pi y}{L} p_2$$

and,

$$\theta(y, t) = \frac{\partial w}{\partial y} = \frac{\pi}{L} \cos \frac{\pi y}{L} p_1 \quad (13)$$

$$\psi(y, t) = -\frac{\partial u}{\partial y} = -\frac{\pi}{L} \cos \frac{\pi y}{L} p_2$$

Using Eq. (12) and Eq. (13) in Eq. (4), the kinetic energy of the disc is given by:

$$T_D = \frac{1}{2} \left[M_D \sin^2 \left(\frac{\pi y}{L} \right) + I_{Dx} \left(\frac{\pi}{L} \right)^2 \cos^2 \left(\frac{\pi y}{L} \right) \right] (\dot{p}_1^2 + \dot{p}_2^2) - I_{Dy} \Omega \left(\frac{\pi}{L} \right)^2 \cos^2 \left(\frac{\pi y}{L} \right) \dot{p}_2 p_1 \quad (14)$$

Using Eq. (12) in Eq. (9), the strain energy of the shaft may be written as:

$$U = \frac{1}{2} \langle EI \rangle \left(\frac{\pi}{L} \right)^4 \left[\int_0^L \sin^2 \left(\frac{\pi y}{L} \right) dy \right] (p_1^2 + p_2^2) \quad (15)$$

The application of the Lagrange's equation in Eq. (14) and (15) leads to:

$$a \ddot{p}_1 + b \Omega \dot{p}_2 + c p_1 = 0 \quad (16)$$

$$a \ddot{p}_2 - b \Omega \dot{p}_1 + c p_2 = 0$$

$$\text{with: } a = \left[M_D \sin^2\left(\frac{\pi}{L}\right) + I_{Dx} \left(\frac{\pi}{L}\right)^2 \cos^2\left(\frac{\pi}{L}\right) \right], b = I_{Dy} \left(\frac{\pi}{L}\right)^2 \cos^2\left(\frac{\pi}{L}\right), c = \langle EI \rangle \left(\frac{\pi}{L}\right)^3 \left(\frac{\pi}{2}\right)$$

The solution for the Eq. (16) are:

$$p_n = P_n e^{rt} \quad (17)$$

where $r = \pm j \omega(\Omega)$ are the natural frequencies in bending on each velocity of rotation of the rotor.

Using Eq. (17) in Eq. (16) we obtain the characteristic equation for the rotor in which the roots are the natural frequencies:

$$r^4 + \left(\frac{2c}{a} + \frac{b^2}{a^2} \Omega^2 \right) r^2 + \frac{c^2}{a^2} = 0 \quad (18)$$

An approach for the displacement in torsion for this configuration is:

$$\varphi(y, t) = (ay). q \quad (19)$$

By replacing Eq. (19) in Eq. (10), the kinetic energy of the shaft is given as:

$$T = \frac{1}{2} \left(\frac{1}{3} J \rho L \right) \dot{q}^2 \quad (20)$$

By Using Eq. (20) in Eq. (13), the strain energy of the shaft is given as:

$$U = \frac{1}{2} \frac{\langle GJ \rangle}{L} q^2 \quad (21)$$

The application of the Lagrange's equation in Eq. (20) and (21) leads to:

$$\omega = \frac{1}{2\pi L} \sqrt{\frac{3 \langle GJ \rangle}{J \rho}} \quad (22)$$

where ω is the natural frequency in torsion of the rotor.

4. HOMOGENEITY PROPERTIES OF THE SHAFT

In Eq. (15) and Eq. (22) we can identify the properties of the cross section of the shaft as the equivalent bending stiffness $\langle EI \rangle$ and the equivalent torsional stiffness $\langle GJ \rangle$. In the case of

rotors in which the shaft are made of fibre/resin in a winding process, the orientation of the winding angle can modify the strain energy of the shaft. So, the Campbell Diagram, can be appreciably changed with the evolution of the orientation of the winding angle.

In this work we use the equivalent stiffness $\langle EI \rangle$ and $\langle GJ \rangle$ as a function of the winding angle for a hollow shaft in kevlar/epoxy and glass/epoxy as shown in Pereira (1999). In this case the external diameter and the internal diameter of the winding-shaft are 40 mm and 32 mm, and the length is 0,8 m. The configuration of the layers in the thickness direction of the shaft is $[\theta, -\theta]_4$.

As demonstrated by Pereira (1999), the equivalent bending stiffness $\langle EI \rangle$ and equivalent torsional stiffness $\langle GJ \rangle$ can be seen in Fig. 4 for a kevlar/epoxy winding-shaft and in Fig. 5 for a glass/epoxy winding-shaft.

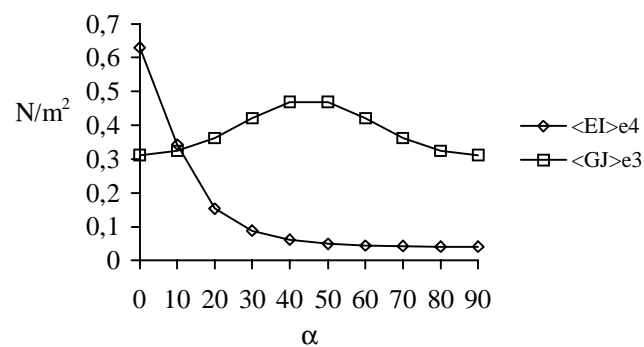


Figure 4 - Evolution of $\langle EI \rangle$ and $\langle GJ \rangle$ as function of the winding angle α – kevlar/epoxy

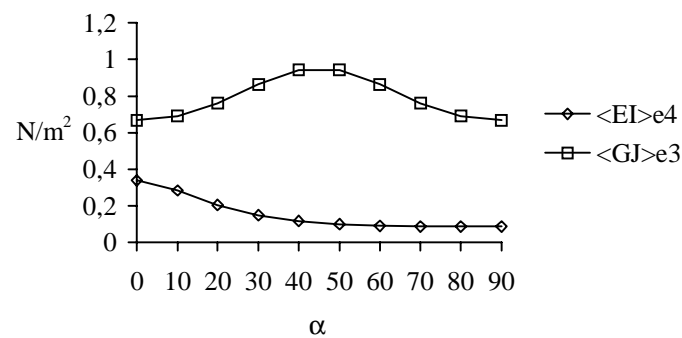


Figure 5 - Evolution of $\langle EI \rangle$ and $\langle GJ \rangle$ as function of the winding angle α – glass/epoxy

5. APPLICATION AND CONCLUSIONS

In this section we plotted the Campbell Diagram for the simple-supported rotor shown in Fig. 3 for different winding angles. The equivalent stiffness $\langle EI \rangle$ and $\langle GJ \rangle$ are from Fig. 4 and from Fig. 5. The properties of the disc are: $I_{Dx} = 0.1225 \text{ kg.m}^2$, $I_{Dy} = 0.245 \text{ kg.m}^2$ and $M_D = 7,85 \text{ kg}$. The bending modes are in full lines and the torsional modes are in dotted lines.

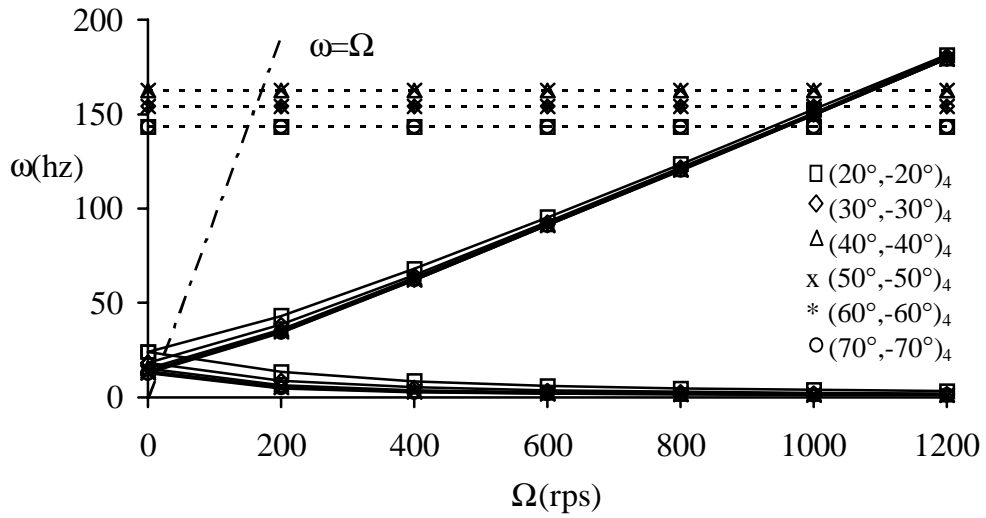


Figure 6 – Campbell Diagram - kevlar/epoxy winding shaft

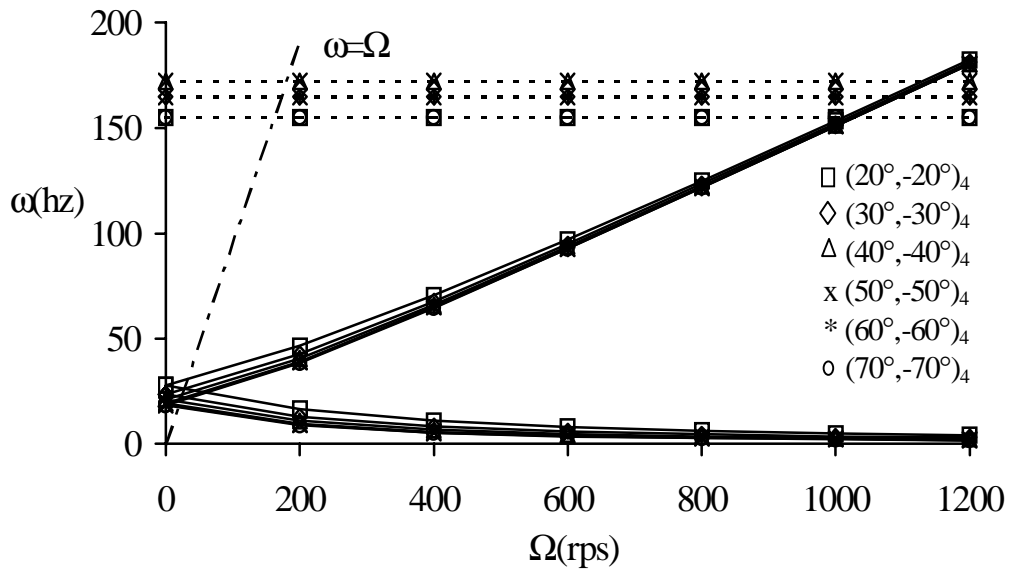


Figure 7 – Campbell Diagram - glass/epoxy winding shaft

This work shows the application of composite materials in rotor dynamics. As we can see in the Fig. 6 and Fig. 7, the Campbell Diagram changes with the orientation of the winding angle. This effect are more appreciably on low velocity of rotation Ω in bending modes. We can also identify a winding angle in which we have the highest distance between the bending modes and the torsional modes on the same velocity of rotation Ω , let be 45° .

Using composite materials in rotor dynamic analysis can introduce additional design variables which may be searched for the optimal performance, as the stiffness and the damping of the material, the winding angle, the number of layers and the weight.

REFERENCES

- Lalanne, M., Berthier, P., Der Hagopian, J., 1986, *Mécanique des vibrations Lineaires*, Masson.
- Nelson, H. D., McVaugh, J. M. 1976, The dynamics of rotor-bearing systems using finite elements, *Journal of Engineering for Industry*, May.
- Pereira, J. C., 1999, A numerical approach on determinig the equivalent torsional stiffness of wounding-tubes, 20th Iberian Latin-American Congress of Computational Methods in Engineering, São Paulo. (a aparecer).
- Rossi, M. A., Squarzoni, A. D., 1986, Finite element modal approach to large rotor-bearing system analysis.
- Özgüven, H. N., Özkan Z. L., 1984, Whril speeds and unbalance response of multibearing rotors usinf finie elemes, *Journal of Vibration, Acoustics, Stress, and Reliability in Design*, Vol. 106, January.
- Steffen Jr., V., Marcelin, J. L., 1987, Dynamic Optimization of Rotors, 9th Brazilian Congress of Mechanical Engineering, Florianópolis.